CASE 11

Particle-Size Adjustment in a Fine Grinding Process for a Developer

Abstract: As a result of a parameter design based on an L_9 orthogonal array using easily changeable factors in a grinding process, we obtained sufficiently good results in the adjustability of particle size. However, since we could not achieve an adequate improvement in particle-size distribution, we tackled our second parameter design with an L_{18} orthogonal array, utilizing more control factors to improve both particle-size adjustment and distribution.

1. Introduction

A prototyping device used in the research stage is a combination of grinding and separating devices, which has the advantages of requiring less material for experiments and enabling us to arrange various factors easily. Using a parameter design based on an L_9 orthogonal array with easily changeable factors in the first experiment, we obtained a sufficiently good result in particle-size adjustability. However, since we could not achieve an adequate improvement in particle-size distribution, we tackled our second parameter design with an L_{18} orthogonal array by taking in more control factors to improve both particle-size adjustment and distribution.

Figure 1 shows the grinding and separating device utilized. At the supply area (1), roughly ground material (sample) is input, and subsequently is dispersed at the cyclone (2) and carried from the separating area to the grinding area. At the separating area, an airflow type of separating machine classifies particles of different diameters by taking advantage of a balance of centrifugal and suction forces. The material transported to the grinding area strikes an impact plate and is crushed into fine particles. In the separating area, only particles of a target size are sorted out; larger granules are reground in the grinding area. Thus, in the grinding and separating process, a granule is pulverized repeatedly until it matches the target size.

Although in our conventional process, we have focused on the separating conditions as the key point for improvement in granular diameter adjustment and distribution, we implemented experiments based primarily on grinding conditions by changing our approach drastically in this research. In addition, we arranged control factor conditions manually that cannot be prepared easily using our current machine, by using ready-made component parts, such as the impact plate, whose shape is regarded to largely affect diameter and distribution. Through reiterative preliminary experiments, we narrowed the control factor levels down to six types of shapes. More important, whereas we have traditionally considered grinding and separating as independent systems, we conducted experiments in this study by considering the two factors together.

2. Ideal Function and SN Ratio

The ideal function at the grinding area is that particle size varies linearly with little variability in grinding energy, which is an adjusting factor. Therefore, as shown in Figure 2, the reciprocal of grinding energy is considered as a signal factor such that the diameter of particles becomes zero when grinding energy approaches infinity, so we proceeded with our analysis based on zero-point proportional SN

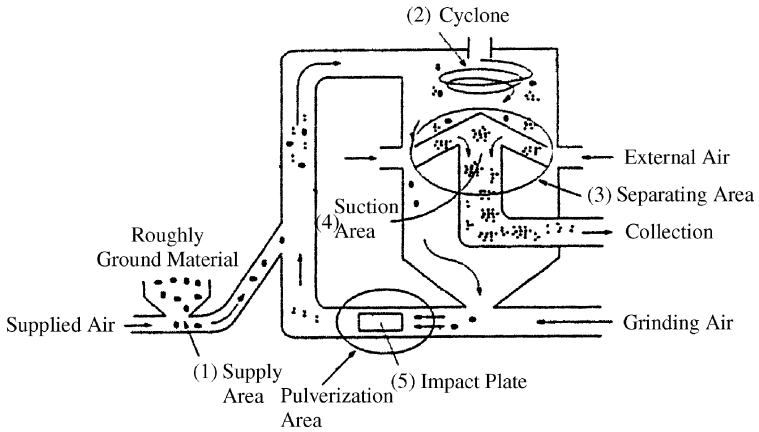

Figure 1
Schematic drawing of grinding and separating device

ratio. For the signal factor, grinding pressure that corresponds to grinding energy was used:

$$M_1: \quad \frac{1}{\text{high pressure}}$$

$$M_2: \quad \frac{1}{\text{medium pressure}}$$

$$M_3: \quad \frac{1}{\text{low pressure}}$$

Choosing the hardness and weight of a sample as noise factors, we termed the level with a larger granular diameter after collection as N_1 (hard and light) and the one with a smaller diameter as N_2 (soft and heavy). The particle-size distribution of ground samples was measured using a Coulter counter, and the data were put in order in a histogram, with particle diameter on the horizontal axis and volumetric percentage on the vertical axis (Figure 3). We calculated the fraction of particles smaller than the average or target diameter from this histogram and used them as the characteristics for analysis in our conventional process. These characteristics are closely related to the quality of photocopy images and reliability. In addition,

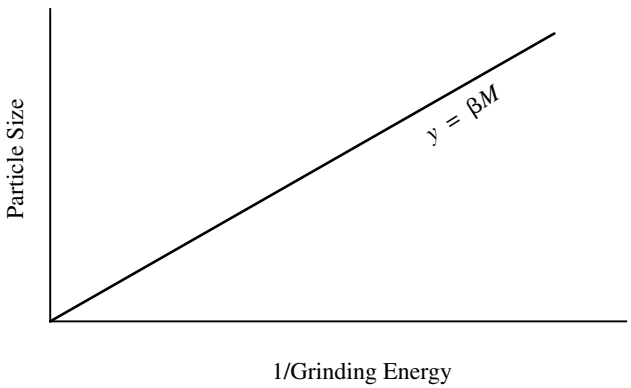

Figure 2
Relationship between grinding energy and particle size

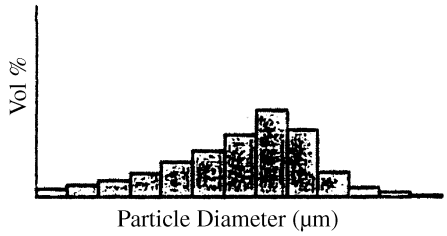

Figure 3
Particle-size distribution after grinding

production capacity and yield have to be considered, so we must make an overall judgment. However, it was quite difficult to satisfy all of them, so in most cases we had to compromise.

In this experiment we needed to compute an average y and variance V from the particle-size distribution data in Figure 3. Primarily, we tabulated the values of particle diameters (x_1, ... , x_{14}) and fractions (p_1, ... , p_{14}):

Measurement channel:

1 2 3 4 ··· 11 12 13 14

Average particle diameter (μm):

x_1 x_2 x_3 x_4 ··· x_{11} x_{12} x_{13} x_{14}

Fraction (%):

p_1 p_2 p_3 p_4 ··· p_{11} p_{12} p_{13} p_{14}

After calculating the average (y) and variance (V) as

$$y = \frac{x_1p_1 + x_2p_2 + \cdots + x_{14}p_{14}}{100} \tag{1}$$

$$V = \frac{x_1^2p_1 + x_2^2p_2 + \cdots + x_{14}^2p_{14}}{100} - y^2 \tag{2}$$

we obtained Table 1. Using these data, we computed a zero-point proportional SN ratio.

Total variation:

$$S_T = (y_{11})^2 + (y_{12})^2 + (y_{13})^2 + (y_{21})^2 + (y_{22})^2 + (y_{23})^2 \tag{3}$$

Effective divider:

$$\gamma = M_1^2 + M_2^2 + M_3^2 \tag{4}$$

Variation of proportional term:

$$S_\beta = \frac{(L_1 + L_2)^2}{2\gamma} \tag{5}$$

Variation of differences between proportional terms:

$$S_{N\beta} = \frac{(L_1 - L_2)^2}{2\gamma} \tag{6}$$

Error variation:

$$S_e = S_T - S_\beta - S_{N\beta} \tag{7}$$

Error variance:

$$V_e = \frac{S_e}{4} \tag{8}$$

Total error variance:

$$V_N = \frac{S_{N\beta}}{5} + S_e + \frac{V_{11} + V_{12} + V_{13} + V_{21} + V_{22} + V_{23}}{6} \tag{9}$$

Table 1
Average particle diameter (y) and variance (V) for each experiment

	M_1	M_2	M_3	Linear Equation
N_1	y_{11} V_{11}	y_{12} V_{12}	y_{13} V_{13}	$L_1 = M_1y_{11} + M_2y_{12} + M_3y_{13}$
N_2	y_{21} V_{21}	y_{22} V_{22}	y_{23} V_{23}	$L_2 = M_1y_{21} + M_2y_{22} + M_3y_{23}$

Table 2
Control factors and levels

Control Factor		Level 1	2	3	4	5	6
A:	type of impact plate	Cone 1	Cone 2	Trapezoid 1	Trapezoid 2	Triangle 1	Triangle 2
B:	distance of impact plate	1.0	1.5	2.0			
C:	amount of material supplied	1.0	1.5	2.0			
D:	supply time	10	20	30			
E:	damper condition	10	25	40			
F:	separating area condition	20	18	16			
G:	particle diameter of supplied material	1.0	1.5	2.0			

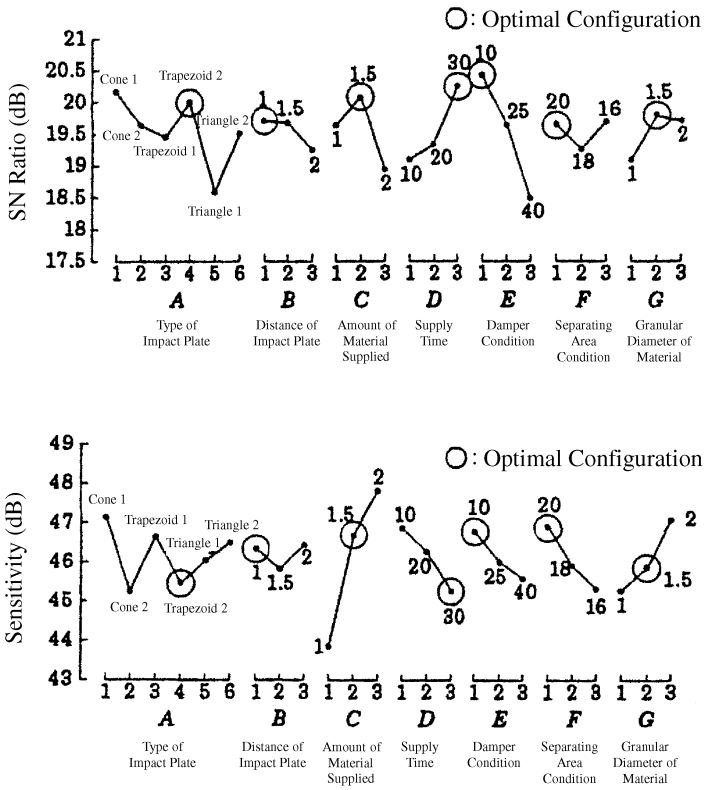

Figure 4
Response graphs

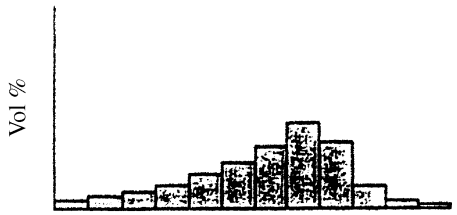

(*a*) Particle-size distribution under current condition

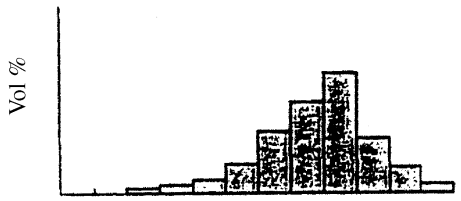

(*b*) Particle-size distribution under L_9 optimal condition

(*c*) Particle-size distribution under L_{18} optimal condition

Figure 5
Improvement in particle-size distribution

SN ratio:

$$\eta = 10 \log \frac{(1/2\gamma)(S_\beta - V_e)}{V_N} \tag{10}$$

Sensitivity:

$$S = 10 \log (1/2\gamma)(S_\beta - V_e) \tag{11}$$

As control factors, we set up A, B, C, D, E, F, and G, as summarized in Table 2.

3. Optimal Configuration and Confirmatory Experiment

Figures 4 and 5 show the response graphs of the SN ratio and sensitivity. Although the optimal configuration based on the SN ratio is $A_1B_1C_2D_3E_1F_1G_2$, we selected A_4 in place of A_1 because A_1's manufacturing conditions were poor and estimated the process average using *A*, *C*, *D*, and *E*.

Estimation of SN ratio

$$\eta = A_4 + C_2 + D_3 + E_1 - 3T = 22.15 \text{ dB} \tag{12}$$

Estimation of sensitivity:

$$S = A_4 + C_2 + F_1 + G_2 - 3T = 46.69 \text{ dB} \tag{13}$$

As a result of the confirmatory experiment, we can see that good reproducibility were achieved for the SN ratio and sensitivity, as summarized in Table 3. As for the current conditions, we estimated the gain using the optimal configuration in the first L_9 experiment. As the difference caused by N_1 and N_2 decreased, we adjusted the particle diameter by fine-adjusting with pressure. That is, with hardly any change in grinding or separating conditions, we

Table 3
Results of confirmatory experiment (dB)

Optimal Configuration	SN Ratio		Sensitivity	
	Estimation	Confirmation	Estimation	Confirmation
L_{18}	22.15	22.19	46.69	46.00
L_9	17.13	17.13	45.29	45.31
Gain	5.02	5.07	1.40	0.69

Table 4
Data for dynamic operating window

Signal Threshold	Error	Grinding Pressure T_1	Grinding Pressure T_2	Grinding Pressure T_3	Linear Equation
M_1	N_1	y_{111}	y_{112}	y_{113}	L_1
	N_2	y_{121}	y_{122}	y_{123}	L_2
M_2	N_1	y_{211}	y_{212}	y_{213}	L_3
	N_2	y_{221}	y_{222}	y_{223}	L_4

converted samples of different sizes and weights into almost identical particles.

As shown in Figure 5, we can change the particle-size distribution under the L_9 optimal configuration into a narrower distribution. Consequently, not only a drastic improvement in yield but also the elimination of fine adjustment of particle diameter were attained. The proportions of small and large particles were reduced significantly under the optimal configuration as compared with those under the current and L_9 optimal configurations, and eventually we obtained an extremely sharp distribution, as illustrated in Figure 5*c*.

4. Analysis Using a Dynamic Operating Window

In the next analysis it was assumed that the relationship between grinding energy, T, and reduction of raw material speed follows equation (16.4), where Y and Y_0 denote the amount of after-ground product and before-ground material, respectively. The grinding efficiency should be highest when the grinding process follows the equation.

$$\frac{Y}{Y_0} = 1 - e^{-\beta T} \tag{14}$$

When performing an analysis based on the dynamic operating window, an important key point is how to determine the portions corresponding to side reactions and underreactions in chemical reactions. Since we produce small particles from raw material in a grinding system, we can assume that a side-reacted part, p, is the part in the particle-size distribution where the particle diameter is smaller than the targeted product, and unreacted part, q, is that where the particle diameter is larger than the targeted product. The objective product is in-between.

Although time is considered a preferable signal factor in a chemical reaction, we have not been able to measure grinding time, due to the technical limitations of this device. Therefore, similar to the situation in zero-point proportional analysis, we computed an SN ratio using grinding pressure as a signal factor.

Now the converted values of p and q were used for the following calculation of SN ratio:

M_1 (small particles):

$$y_1 = \ln \frac{1}{1-p}, \qquad 1 - p = \frac{Y_1}{Y_0} \tag{15}$$

M_2 (large particles):

$$y_2 = \ln \frac{1}{q}, \qquad q = \frac{Y_2}{Y_0} \tag{16}$$

All data obtained are shown in Table 4. The SN ratio is computed as follows:

Total variation:

$$S_T = y_{111}^2 + y_{112}^2 + \cdots + y_{223}^2 \qquad (f = 12) \tag{17}$$

Variation of proportional term:

$$S_\beta = \frac{(L_1 + \cdots + L_4)^2}{4\gamma} \qquad (f = 1) \tag{18}$$

Variation of proportional terms due to M:

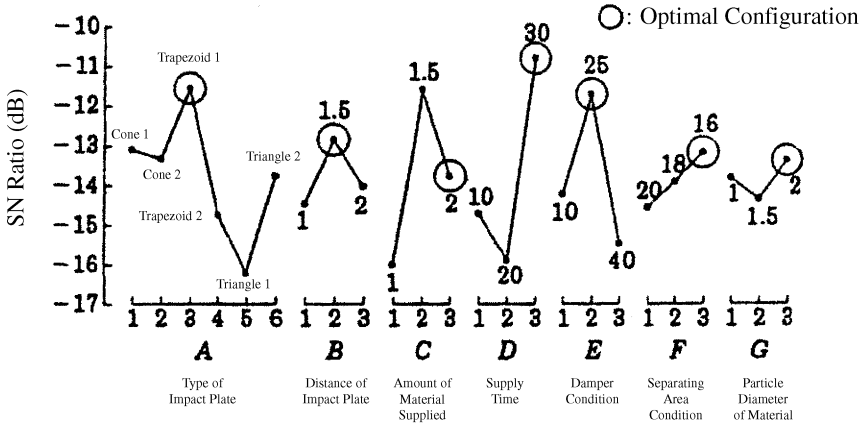

(*a*) SN Ratio, η, of Operating Window

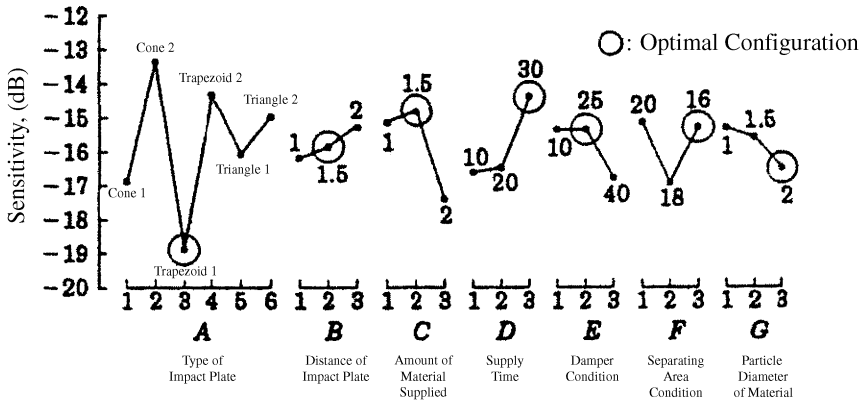

(*b*) Sensitivity, *S**, in Operating Window

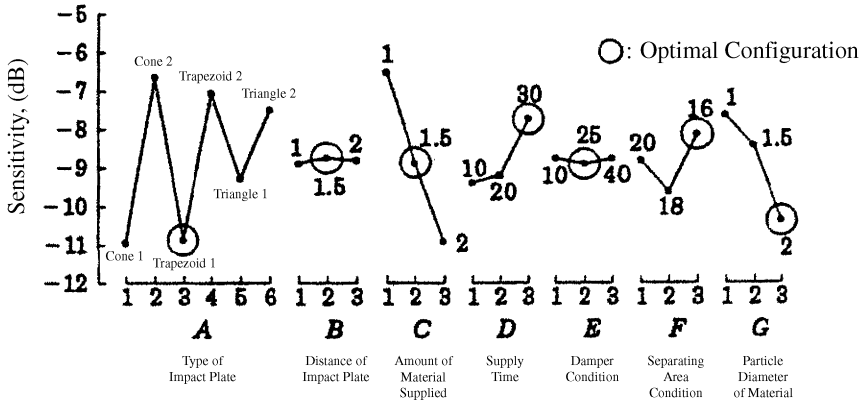

(*c*) Sensitivity, *S*

Figure 6
Response graphs of dynamic operating window

$$S^*_{M\beta} = \frac{(L_1 + L_2)^2 + (L_3 + L_4)^2}{2\gamma} - S_\beta \qquad (f = 1) \tag{19}$$

Variation of proportional terms due to N:

$$S^*_{N\beta} = \frac{(L_1 + L_3)^2 + (L_2 + L_4)^2}{2\gamma} - S_\beta \qquad (f = 1) \tag{20}$$

Error variation:

$$S_e = S_T - S_\beta - S^*_{M\beta} - S^*_{N\beta} \qquad (f = 9) \tag{21}$$

Error variance:

$$V_e = \frac{S_e}{9} \tag{22}$$

Total variance:

$$V_N = \frac{S_e + S^*_{N\beta}}{10} \tag{23}$$

SN ratio of operating window:

$$\eta = 10 \log \frac{(1/4\gamma)(S^*_{M\beta} - V_e)}{V_N} \tag{24}$$

Sensitivity:

$$S = 10 \log \frac{1}{4\gamma} (S_\beta - V_e) \tag{25}$$

Sensitivity of operating window:

$$S^* = 10 \log \frac{1}{4\gamma} (S^*_{M\beta} - V_e) \tag{26}$$

Figure 6 illustrates the response graphs for the SN ratio and sensitivity. Since factor levels with a high SN ratio are optimal, we prepared our estimates under the optimal configuration selected.

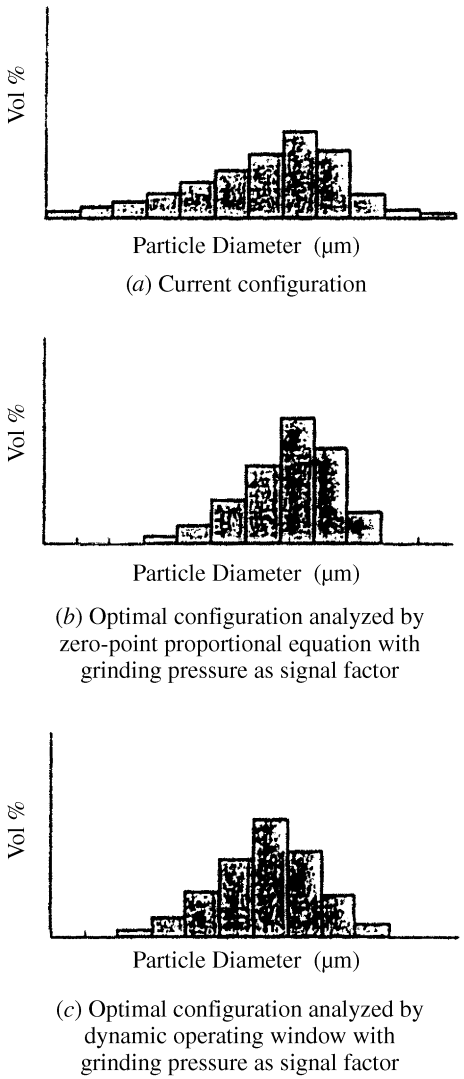

Figure 7
Comparison of particle-size distribution

Table 5
Confirmation by dynamic operating window method

	Estimation	Confirmation
SN ratio of operating window	−9.97	−11.53
Sensitivity of operating window, S	−6.76	−5.75
Sensitivity of operating window, S^*	−11.36	−10.59

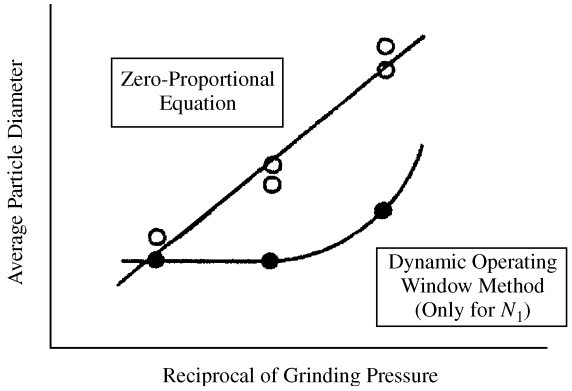

Figure 8
Relationship between grinding pressure and particle diameter

5. Optimal Configuration and Confirmatory Experiment

A confirmatory experiment under the optimal configuration could not be performed because only test samples for N_1 have remained. Then, using the optimal configuration grounded on the aforementioned zero-point proportional equation and the data for a granular diameter distribution in its confirmatory experiment, we computed the SN ratio and sensitivity and checked the reproducibility. The result is summarized in Table 5, which reveals that fairly good reproducibility of the SN ratio and sensitivity was obtained.

As a next step, using only test samples for N_1, we ground actual material under the optimal configuration. For all of the results under the initial, zero-point proportional–based optimal, and dynamic operating window–based optimal configurations, the particle diameter distribution for the N_1 sample is illustrated in Figure 7. Under each condition, the particle size distribution was different. But the figure shows that the conditions for the two optimal configurations (except the current configuration) can be used for mass production.

Next, we checked the particle diameter adjustability under the optimal configuration based on the dynamic operating window, as shown in Figure 8. Compared with that under the optimal configuration using the zero-point proportional equation, adjustability using grinding pressure worsened.

Considering all of the above, we can summarize the dynamic operating window characteristics as follows:

1. When using the dynamic operating window method, the particle-size distribution was horizontally symmetrical, as shown in Figure 7*c*. Although this tendency was not regarded as problematic, but as rather good, we need to further separate the particles because of the broad distribution.
2. As compared to that under the optimal configuration using a zero-point proportional equation, the grinding efficiency improved significantly. In other words, if we grind under the same pressure, we can obtain a condition where we can make the particles smaller.
3. Despite the improvement noted above, the particle-size adjustability was poorer. This indicates that we achieved the results as defined in equation (14).
4. Our experiment proves that a dynamic operating window method can also be used in nonchemical reaction areas.
5. According to the results shown in Figure 8, grinding time should be chosen as a signal factor rather than using grinding pressure.

References

Hiroshi Shibano, Tomoharu Nishikawa, and Kouichi Takenaka, 1994. Establishment of particle size adjusting technique for a fine grinding process for developer. *Quality Engineering*, Vol. 2, No. 3, pp. 22–27.

Hiroshi Shibano, Tomoharu Nishikawa, and Kouichi Takemaka, 1997. Establishment of control technique for particle size in roles of fine grinding process for developer. *Quality Engineering*, Vol. 5, No. 1, pp. 36–42.

This case study is contributed by Hiroshi Shibano.